Chapter 13
Output-Only Modal Parameter Estimation Using a Continuously Scanning Laser Doppler Vibrometer System with Application to Structural Damage Detection

Y. F. Xu, Da-Ming Chen, and W. D. Zhu

Abstract Spatially dense vibration measurement can be obtained by use of a continuously scanning laser Doppler vibrometer (CSLDV) system that sweeps its laser spot along a scan path. For a linear, time-invariant, viscously damped structure undergoing free vibration, a new type of vibration shapes called free response shapes was defined and obtained by the authors using a CSLDV system with the demodulation method. To date, application of free response shapes is limited to structural damage identification, and they cannot be directly used for model validation while mode shapes can be. This paper extends the concept of free response shapes by proposing a new output-only modal parameter estimation (OMPE) method using a CSLDV system to estimate modal parameters of the structure undergoing free vibration, including natural frequencies, modal damping ratios, and mode shapes. Advantages of the proposed method are: (1) modal damping ratios and mode shapes can be accurately estimated from obtained free response shapes, (2) the scanning frequency of the CSLDV system can be relatively low, and (3) estimated mode shapes can be used for structural damage identification as if they were measured by stepped scanning of a scanning laser Doppler vibrometer. A baseline-free method is applied to identify structural damage using mode shapes estimated by the proposed OMPE method. The analytical expression of free response shapes of the structure is derived, based on which the OMPE method is proposed and presented as a step-by-step procedure. In the proposed OMPE method, natural frequencies of the structure are identified from free response of certain fixed points on the structure; its modal damping ratios and mode shapes are simultaneously estimated using free response shapes measured by a CSLDV system. A numerical investigation is conducted to study the OMPE method and its application to baseline-free damage identification with mode shapes estimated by the OMPE method.

Keywords Continuously scanning laser Doppler vibrometer system · Modal parameter estimation · Output-only method · Baseline-free structural damage identification · Demodulation method

13.1 Introduction

Vibration-based damage identification has been a major research topic of structural dynamics in the past few decades [1, 2]. More than often, occurrence of damage in a structure undermines its capability of supporting design loads and can result in its excessive deformation, which is attributed to changes in its structural properties, such as its stiffness. One assumption of a vibration-based damage identification method is that occurrence of damage changes modal parameters of a structure, including natural frequencies, modal damping ratios, and mode shapes, which can be accurately estimated by modal analysis [3]. Accurately estimated modal parameters can also assist model validation and updating. A continuously scanning laser Doppler vibrometer (CSLDV) system is an ideal instrument for modal parameter estimation as it is capable of accurate, non-contact and temporally dense vibration measurement and also capable of spatially dense mode shape measurement [4]. A CSLDV system consists of three key components: a laser Doppler vibrometer, a scanner and a controller [5]. The vibrometer measures the velocity of a point on a test structure where its laser spot is located. The laser beam of the vibrometer is directly shined onto first-surface mirrors of the scanner and the spot is continuously swept along a prescribed scan path

Y. F. Xu
Department of Mechanical and Materials Engineering, University of Cincinnati, Cincinnati, OH, USA
e-mail: xu2yf@uc.edu

D.-M. Chen · W. D. Zhu (✉)
Department of Mechanical Engineering, University of Maryland, Baltimore, MD, USA
e-mail: damingc1@umbc.edu; wzhu@umbc.edu

C. Niezrecki et al. (eds.), *Rotating Machinery, Optical Methods & Scanning LDV Methods, Volume 6*, Conference Proceedings of the Society for Experimental Mechanics Series, https://doi.org/10.1007/978-3-030-12935-4_13

on the structure by rotating the mirrors that are controlled by the controller. While the spot is continuously swept, velocity at each discrete measurement point on the scan path is measured, and the number of the measurement points can be tens and even hundreds of thousands, depending on the sampling and scan frequencies of the vibrometer. A CSLDV system has been successfully used for modal analysis and measurements of vibration shapes, such as mode shapes [6–8] and operating deflection shapes [9–11], which can be achieved with high accuracy and in a relatively short time, e.g., in a few seconds. Specifically, two operational modal analysis methods [12, 13] have been developed based on harmonic power spectra [14], where only one CSLDV system is used to measure response of a structure under environmental excitation without any additional sensors, and modal parameters of a wind turbine blade were measured [12, 13].

A CSLDV system has been used to measure high-fidelity vibration shapes of structures undergoing steady-state vibrations for damage identification [5, 15], and the vibration shapes measured by a CSLDV system can be used to identify structural damage as small as notch-size ones [16]. A new type of vibration shapes called free response shapes was defined and measured by a CSLDV system when a linear underdamped beam underwent free vibration [17]. Free response shapes were used to identify structural damage, where damage indices associated with multiple elastic modes of a beam could be obtained. The free response shapes can be considered to be obtained in an output-only manner, since initial conditions of and excitation given to the beam do not need to be measured. A free response shape is different from a mode shape, since the former is time-varying with decaying amplitudes and the latter is not. So far, application of free response shapes is limited to structural damage identification and they cannot be directly used for model validation and updating due to two reasons. One is that a free response shape has an amplitude that is determined by excitation. Unless one can accurately measure the excitation, a free response shape cannot be used for model validation and updating. Another reason is that damping ratios cannot be estimated from free response shapes that are obtained in the method in Ref. [17]. An experimental modal analysis method was proposed [8], where excitation to a test structure and its free response measured by a CSLDV system yielded pseudo-frequency response functions of the structure, which were used to estimate modal parameters of the structure. In this method, the measured response is lifted to each measurement point as if the response were measured in a pointwise manner. A limitation of the method is that measured mode shapes of modes with relatively high natural frequencies can have low qualities due to speckle noise caused by a relatively high scanning frequency, which is needed since the scanning frequency of the CSLDV system is equal to the sampling frequency of the lifted response at each measurement point. While operational modal analysis methods using a CSLDV system have been proposed and their capabilities of modal parameter estimation have been experimentally validated, their resulting mode shapes and associated curvature mode shapes cannot be used for structural damage identification. The reason is that the resulting mode shapes are represented by smooth sinusoidal functions [12, 13] and local anomalies caused by existing local structural damage cannot be reflected in the mode shapes and associated curvature mode shapes.

In this work, derivation of free response shapes of a linear, time-invariant, viscously damped structure undergoing free vibration is shown. A new output-only modal parameter estimation (OMPE) method using free response measured by a CSLDV system is proposed to accurately estimate modal parameters of the structure with a step-by-step procedure. The proposed OMPE method extends the concept of free response shapes of the structure as they are directly related to its modal damping ratios and mode shapes, which can be simultaneously obtained in the proposed method. A baseline-free non-model-based damage identification method is applied to identify structural damage in a structure. In the identification method, a curvature damage index (CDI) is obtained by comparing a curvature mode shape corresponding to a mode shape estimated by the OMPE method with that from a polynomial that fits the estimated mode shape with a properly determined order. Structural damage can be identified in neighborhoods with consistently large CDIs corresponding to multiple modes. A numerical investigation is conducted to study the OMPE method and application of the damage identification method.

The remaining part of this paper is outlined as follows. Derivation of free response shapes is presented in Sects. 13.2.1 and 13.2.2, the new OMPE method using a CSLDV system is proposed in Sect. 13.2.3, and the structural damage identification method is presented in Sect. 13.2.4. A numerical investigation of the OMPE method and baseline-free method are presented in Sect. 13.3. Finally, conclusions of this study is presented in Sect. 13.4.

13.2 Methodology

13.2.1 Free Response of a Damped Structure

Free response in the form of the displacement of a linear, time-invariant, viscously damped structure can be obtained by solving its governing partial differential equation:

$$B\left[\frac{\partial^2 z(\mathbf{x},t)}{\partial^2 t}\right] + C\left[\frac{\partial z(\mathbf{x},t)}{\partial t}\right] + L\left[z(\mathbf{x},t)\right] = 0, \qquad \mathbf{x}\in D, \qquad t\geq 0 \tag{13.1}$$

where $B(\cdot)$, $C(\cdot)$ and $L(\cdot)$ are a mass operator, a damping operator and a stiffness operator, respectively, z is the displacement of the structure at the spatial position $\mathbf{x}$ at time t, and D is its spatial domain. Boundary and initial conditions of the structure are known. Note that the initial conditions can be induced by an external force that the structure is subject to when $t < 0$. A solution to Eq. (13.1) can be obtained using the expansion theorem [18]:

$$z(\mathbf{x},t) = \sum_{i=1}^{\infty} \boldsymbol{\phi}_i(\mathbf{x})\, u_i(t) \tag{13.2}$$

where $\boldsymbol{\phi}_i$ is the i-th mass-normalized eigenfunction of the associated undamped structure, which is assumed to be self-adjoint, and u_i is the corresponding unknown time function. Orthonormality between $\boldsymbol{\phi}_i$ and $\boldsymbol{\phi}_j$ $(j = 1,\ 2,\ \ldots,\ \infty)$ with respect to B is expressed by

$$\int_D \boldsymbol{\phi}_j(\mathbf{p})\, B\left[\boldsymbol{\phi}_i(\mathbf{p})\right] \mathrm{d}\mathbf{p} = \delta_{ij} \tag{13.3}$$

where δ_{ij} denotes Kronecker delta function, which satisfies $\delta_{ij} = 1$ if $i = j$ and $\delta_{ij} = 0$ if $i \neq j$. Assuming that damping of the structure can be modeled by Kelvin-Voigt viscoelastic model, which leads to a classically damped system [18, 19], one can obtain u_i in Eq. (13.2) by solving an ordinary differential equation:

$$\ddot{u}_i(t) + 2\zeta_i\omega_i\dot{u}_i(t) + \omega_i^2 u_i(t) = 0 \tag{13.4}$$

where ω_i is the corresponding i-th undamped natural frequency of the structure, ζ_i is the i-th modal damping ratio, which is smaller than 1 for an underdamped structure, and an overdot denotes differentiation with respect to t. The initial conditions $u_i(0)$ and $\dot{u}_i(0)$ can be determined from the initial conditions of Eq. (13.1). The solution to Eq. (13.4) can be expressed by [20]

$$\begin{aligned} u_i(t) &= \mathrm{e}^{-\omega_i\zeta_i t}\left[u_i(0)\cos\left(\omega_{i,d}t\right) + \tfrac{\dot{u}_i(0)+\omega_i\zeta_i u_i(0)}{\omega_{i,d}}\sin\left(\omega_{i,d}t\right)\right] \\ &= A_i\mathrm{e}^{-\omega_i\zeta_i t}\cos\left(\omega_{i,d}t - \gamma_i\right) \end{aligned} \tag{13.5}$$

where

$$\omega_{i,d} = \omega_i\sqrt{1-\zeta_i^2} \tag{13.6}$$

is the i-th damped natural frequency of the structure,

$$A_i = \sqrt{\left[u_i(0)\right]^2 + \left[\frac{\dot{u}_i(0) + \omega_i\zeta_i u_i(0)}{\omega_{i,d}}\right]^2} \tag{13.7}$$

is an amplitude constant, and

$$\gamma_i = \operatorname{arctan2}\left(\frac{\dot{u}_i(0) + \omega_i\zeta_i u_i(0)}{\omega_{i,d}},\, u_i(0)\right) \tag{13.8}$$

is a phase angle; $\omega_i\zeta_i$ in Eq. (13.5) is referred to as the decaying rate of u_i. Based on Eqs. (13.2) and (13.5), Eq. (13.2) becomes

$$z(\mathbf{x},t) = \sum_{i=1}^{\infty} A_i\phi_i(\mathbf{x})\,\mathrm{e}^{-\omega_i\zeta_i t}\cos\left(\omega_{i,d}t - \gamma_i\right) \tag{13.9}$$

13.2.2 Free Response Shapes

A free response shape associated with the i-th mode of the structure can be defined by

$$y_i\left(\mathbf{x},t\right)=A_i\phi_i\left(\mathbf{x}\right)\mathrm{e}^{-\omega_i\zeta_i t} \tag{13.10}$$

and Eq. (13.9) becomes

$$z\left(\mathbf{x},t\right)=\sum_{i=1}^{\infty}y_i\left(\mathbf{x},t\right)\cos\left(\omega_{i,d}t-\gamma_i\right) \tag{13.11}$$

The i-th eigenfunction ϕ_i that is the i-th undamped mode shape of the structure exists in the definition of y_i in Eq. (13.10). A similarity between ϕ_i and y_i is that they both correspond to the i-th mode of the structure; however, the former is time-invariant while the latter is time-varying due to the term $\mathrm{e}^{-\omega_i\zeta_i t}$ in Eq. (13.10).

A CSLDV system continuously sweeps its laser spot over a surface of a structure with a specific scan path. The system measures response of a measurement point on the structure with a certain sampling frequency, where its laser spot is located during a scan, and a finite number of modes of the structure are included in free response measured by the system. Let $\tilde{\mathbf{x}}\left(t\right)$ be the position of a laser spot on the surface of the structure at time t, which describes the scan path on the structure as a function of t. Free response of the structure measured by the CSLDV system along $\tilde{\mathbf{x}}\left(t\right)$ can be expressed by

$$\tilde{z}\left(t\right)=\sum_{i=1}^{N}\tilde{y}_i\left[\tilde{\mathbf{x}}\left(t\right),t\right]\tilde{u}_i\left(t\right) \tag{13.12}$$

where N is the number of modes included in $\tilde{z}$, and $\tilde{y}_i$ and $\tilde{u}_i$ are the free response shape and time function associated with the i-th mode measured by the system, respectively. The free response shape $\tilde{y}_i$ in Eq. (13.12) can be written as

$$\tilde{y}_i\left[\tilde{\mathbf{x}}\left(t\right),t\right]=A_i\phi_i\left[\tilde{\mathbf{x}}\left(t\right),t\right]\mathrm{e}^{-\omega_i\zeta_i t} \tag{13.13}$$

The time function $\tilde{u}_i$ can be expressed by

$$\tilde{u}_i\left(t\right)=\cos\left(\omega_{i,d}t-\alpha_i-\theta_i\right) \tag{13.14}$$

where α_i is the difference between the phase determined by the initial conditions and force associated with the i-th mode and that by a mirror feedback signal, and θ_i is a phase variable that controls amplitudes of in-phase and quadrature components of $\tilde{y}_i$, which can be expressed by

$$\tilde{y}_{I,i}=\tilde{y}_i\left[\tilde{\mathbf{x}}\left(t\right),t\right]\cos\left(\alpha_i+\theta_i\right) \tag{13.15}$$

and

$$\tilde{y}_{Q,i}=\tilde{y}_i\left[\tilde{\mathbf{x}}\left(t\right),t\right]\sin\left(\alpha_i+\theta_i\right) \tag{13.16}$$

respectively [5]. The demodulation method has been used to obtain $\tilde{y}_i$ corresponding to each half-scan period by the system [17]. A half-scan period starts when the laser spot of the system arrives at one end of a scan path and ends when the laser spot arrives at the other end of the scan path. Multiple $\tilde{y}_i$ can be obtained from free response of the structure measured by the system in one scan. To identify the start and end of a half-scan period, one can refer to mirror feedback signals of the system and determine instants when its laser spot arrives at ends of a scan path.

13.2.3 OMPE Method

The amplitude of $\tilde{y}_i$ in Eq. (13.13) is time-varying and exponentially decays to zero with t at the decaying rate $\omega_i\zeta_i$. In order to obtain a non-zero amplitude of $\tilde{y}_i$ from the demodulation method, one needs to determine natural frequencies of the structure and instants when the amplitude of $\tilde{y}_i$ decays to zero. The natural frequencies can be determined from the auto-power spectrum of z at a point that is measured by the system, and the instants can be determined using the short-time Fourier transform of $\tilde{z}$ [21], which is denoted by $\tilde{V_w}$. Some details of the short-time Fourier transform can be found in "Appendix: Short-Time Fourier Transform". Multiple non-zero $\tilde{y}_i$ can be obtained by using $\tilde{z}$ of the first $N_{i,0}$ half-scan periods, where $N_{i,0}$ is an integer that is defined by

$$\arg\max_{N_{i,0}} \frac{N_{i,0}T}{2} \leq t_{i,0} - t_1 \tag{13.17}$$

in which T is the length of a scan period, $t_{i,0}$ is the instant when $\tilde{V_w}$ at the i-th natural frequency of the structure becomes almost zero, and t_1 is the instant when the first half-scan period starts.

Let

$$Q_i = A_i \mathrm{e}^{-\omega_i\zeta_i t_1} \tag{13.18}$$

which is a complex constant, and $Q_i\phi_i$ can also represent the i-th mode shape of the structure. One has $Q_i = A_i$ when $t_1 = 0$, and Eq. (13.13) with $t \geq t_1$ can be expressed by

$$\tilde{y}_i\left[\tilde{\mathbf{x}}(t), t\right] = Q_i\phi_i\left[\tilde{\mathbf{x}}(t), t\right]\mathrm{e}^{-\omega_i\zeta_i(t-t_1)} \tag{13.19}$$

One can estimate $Q_i\phi_i$ in Eq. (13.19) if ζ_i is known. Let t_k be the instant when the k-th half-scan period starts and $\tilde{y}_{i,k}$ be the free response shape associated with the i-th mode in the k-th half-scan period. The term $Q_i\phi_i$ in Eq. (13.19) associated with $\tilde{y}_{i,k}$ is independent of t and can be estimated by eliminating $\mathrm{e}^{-\omega_i\zeta_i(t-t_1)}$ in $\tilde{y}_{i,k}$; it can be expressed by

$$Q_{i,k}\phi_{i,k}\left[\tilde{\mathbf{x}}(t), t\right] = \tilde{y}_{i,k}\left[\tilde{\mathbf{x}}(t), t\right]\mathrm{e}^{\omega_i\zeta_i(t-t_1)} \tag{13.20}$$

where $0 \leq t - t_k \leq T$. The mean of $Q_{i,k}\phi_{i,k}$ with $k \in [1, N_i]$, where $N_i \leq N_{i,0}$, can be defined by

$$\mu_i\left(\tilde{\mathbf{x}}\right) = \frac{\sum_{k=1}^{N_i} Q_{i,k}\phi_{i,k}\left(\tilde{\mathbf{x}}\right)}{N_i} \tag{13.21}$$

Though $\omega_i\zeta_i$ in Eqs. (13.19) and (13.20) is unknown, it can be estimated by solving an optimization problem:

$$\overline{\omega_i\zeta_i} = \arg\min_{\omega_i\zeta_i} \sum_{k=1}^{N_i} \left|\mu\left(\tilde{\mathbf{x}}\right) - Q_{i,k}\phi_{i,k}\left(\tilde{\mathbf{x}}\right)\right| \tag{13.22}$$

where $|\cdot|$ denotes the L^2-norm of a function in a half-scan period. Note that N_i must be greater than two; otherwise $\omega_i\zeta_i$ cannot be estimated since the problem in Eq. (13.22) becomes trivial. With estimated $\omega_{i,d}$ and $\overline{\omega_i\zeta_i}$, ζ_i can be estimated by

$$\zeta_i = \frac{\overline{\omega_i\zeta_i}}{\sqrt{\omega_{i,d}^2 + \left(\overline{\omega_i\zeta_i}\right)^2}} \tag{13.23}$$

This completes theoretical derivation of the OMPE method using free response of the structure measured by the CSLDV system. The procedure of the method is summarized below:

Step 1. Measure $z(t)$ of the structure using the system with its laser spot staying at least one fixed point of the structure.
Step 2. Estimate $\omega_{i,d}$ of the structure using the auto-power spectrum of z measured in Step 1.
Step 3. Measure $\tilde{z}(t)$ using the system along a scan path with certain scan and sampling frequencies.

Step 4. Estimate $\tilde{y}_i\left(\tilde{\mathbf{x}}\right)$ associated with measured modes in N_i half-scan periods using the demodulation method.
Step 5. Estimate ζ_i based on Eq. (13.23) using $\overline{\omega_i\zeta_i}$ obtained by solving the optimization problem in Eq. (13.22).
Step 6. Express $Q_i\phi_i\left(\tilde{\mathbf{x}}\right)$ as $\tilde{y}_{i,1}\left(\tilde{\mathbf{x}}\right)\mathrm{e}^{\overline{\omega_i\zeta_i}(t-t_1)}$ with $0\le t-t_1\le T$ and $\overline{\omega_i\zeta_i}$ obtained in Step 5.

13.2.4 Baseline-Free Structural Damage Identification

Local damage of a structure can cause prominent anomalies in its curvature mode shapes in neighborhoods of the damage, and the damage can be identified by comparing the curvature mode shapes with those of the associated undamaged structure [22]. However, the curvature mode shapes of the undamaged structure that can be considered as baselines are usually unavailable in practice. When the undamaged structure is geometrically smooth and made of materials without mass and/or stiffness discontinuities, the curvatures of the undamaged structure can be well approximated by those from polynomials that fit mode shapes of the damaged structure with properly determined orders. In previous works [15, 16, 23], a curvature damage index (CDI) was proposed, which consists of the difference between a curvature mode shape of a damaged structure and that from a polynomial fit:

$$\delta_i\left(\mathbf{x}\right)=\left[\boldsymbol{\phi}_i''\left(\mathbf{x}\right)-\boldsymbol{\phi}_i^{p''}\left(\mathbf{x}\right)\right]^2 \tag{13.24}$$

where a prime denotes spatial differentiation with respect to the arc length s of a scan path at $\mathbf{x}$, and $\boldsymbol{\phi}_i^p$ is the corresponding mode shape from the polynomial that fits ϕ_i. Since mode shapes corresponding to multiple modes can be measured in one scan, CDIs corresponding to multiple modes can be obtained in the scan, and damage regions can be identified in neighborhoods with consistently large CDI values associated with the measured modes. Note that use of δ_i corresponding to rigid-body modes of a structure should be excluded in damage identification as their curvature mode shapes are zero, and one should use δ_i corresponding to elastic modes of the structure in damage identification. An auxiliary CDI associated with δ_i corresponding to various measured modes can be defined to assist identification of the neighborhoods; it can be expressed by

$$\tilde{\delta}\left(\mathbf{x}\right)=\sum\hat{\delta}_i\left(\tilde{x}\right) \tag{13.25}$$

where $\hat{\delta}_i$ is a normalized CDI associated with the i-th mode of the structure with the maximum unit amplitude and $\sum$ denotes summation of $\hat{\delta}_i$ over all measured modes. Since boundary distortions would occur in curvature free response shapes of a structure associated with its free response shapes obtained from the demodulation method [17], similar distortions would occur in curvature mode shapes here. Hence, boundary regions are excluded in normalization of δ_i in $\tilde{\delta}$ and presenting them. Neighborhoods with consistently large values of δ_i associated with measured modes can be identified in those with large values of $\tilde{\delta}$.

By nondimensionalizing s so that it ranges between -1 and 1, a polynomial that fits ϕ_i with an order r can be expressed by

$$\phi_i^p\left(\tilde{s}\right)=\sum_{q=0}^{r}a_q\tilde{s}^q \tag{13.26}$$

where $\tilde{s}$ denotes the nondimensionalized s, a_q are coefficients of the polynomial. As pointed out in Ref. [17], an increase of r in the polynomial in Eq. (13.26) can improve the level of approximation of ϕ_i^p to ϕ_i. To determine a proper order of the polynomial fit, the modal assurance criterion (MAC) value between a mode shape of the damaged structure and that from a polynomial that fits the mode shape, which is defined by

$$\mathrm{MAC}\left(\phi_i,\phi_i^p\right)=\frac{\left(\phi_i^{\mathrm{H}}\phi_i^p\right)^2}{\left(\phi_i^{\mathrm{H}}\phi_i\right)\left(\phi_i^{p\mathrm{H}}\phi_i^p\right)}\times 100\% \tag{13.27}$$

where the superscript H denotes matrix Hermitization, is used. A proper order for the polynomial fit is two plus the minimum order with which $\mathrm{MAC}\left(\phi_i,\phi_i^p\right)$ is greater than 90% [23]. Two is added here in order to preserve smoothness of a curvature mode shape from the polynomial fit, since calculation of a curvature incurs second-order differentiation that reduces the order of a polynomial by two.

13.3 Numerical Investigation

A finite element model of a damaged aluminum cantilever beam with a length $L = 0.8$ m, Young's modulus of 68.9 GPa, a mass density of 2700 kg/m^3 and a damping coefficient of Kelvin-Voigt damping model of 8×10^{-7} s is constructed using ABAQUS. The beam has a uniform square cross-section with a side length of 0.01 m. The damage is in the form of thickness reduction, which is located between $x = \frac{6}{16}L$ and $x = \frac{7}{16}L$, where x is the position of a point on the beam. The damaged portion of the beam has a height of 0.008 m and a length of 0.05 m. The beam has fixed and free ends at $x = 0$ and $x = L$, respectively. The first five natural frequencies and modal damping ratios of the beam are listed in Table 13.1a, b, respectively. The first five mass-normalized mode shapes of the beam from its finite element model are shown in Fig. 13.1.

In this section, a single impulse is applied to the damaged cantilever beam. Assume that the beam has zero initial conditions; responses of the beam are calculated using the expansion theorem, where the number of included modes is five. A simulated CSLDV system is used to measure responses of the beam caused by the forces with a scan period $T = 2$ s and a sampling frequency of 16384 Hz. The simulated CSLDV system is capable of measuring response in the form of displacement. Positions of the laser spot of the system on the beam in the first eight seconds of a scan is shown in Fig. 13.2.

A single impulse with an intensity of 0.01 Ns is applied to the free end of the damaged beam $x = L$ at $t = 0$ s. Response of the beam at $x = 0.7$ m is measured in the form of displacement for eight seconds, as shown in Fig. 13.3a, and its auto-power spectrum is shown in Fig. 13.3b. Natural frequencies of the beam can be identified in the spectrum as frequencies where prominent peaks are found, and identified natural frequencies are listed in Table 13.1a. The largest error between the identified natural frequencies and those from the finite element model is 0.16%. Response of the beam is then measured using the simulated CSLDV system, and the measured response in the first eight seconds are shown in Fig. 13.4a; the associated

Table 13.1 First five (a) natural frequencies in Hz and (b) modal damping ratios in percentage of the damaged beam from its finite element model and the OMPE method using its response caused by a single impulse

(a)

Mode	Finite element	OMPE method
1	12.64	12.62
2	79.04	79.00
3	222.0	222.0
4	434.8	434.7
5	711.2	711.2

(b)

Mode	Finite element	OMPE method
1	0.0032	0.0032
2	0.0199	0.0199
3	0.0558	0.0558
4	0.1093	–
5	0.1787	–

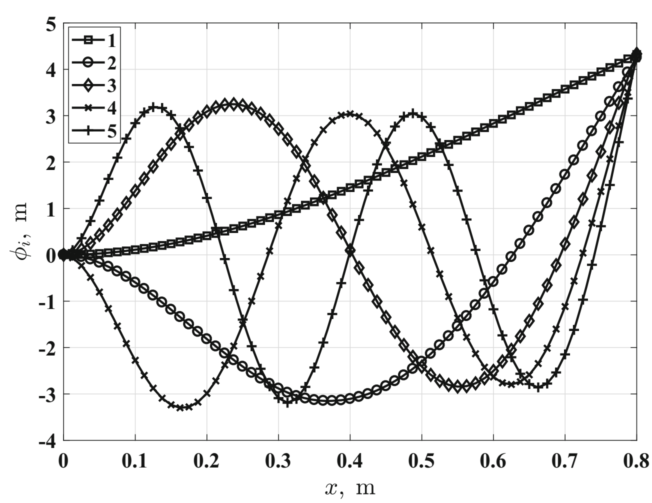

Fig. 13.1 Mass-normalized mode shapes of the damaged cantilever beam associated with its first five modes from its finite element model

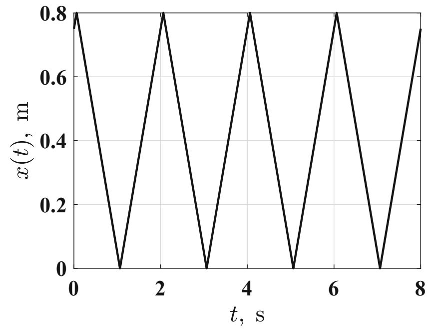

Fig. 13.2 Position of the laser spot of the simulated CSLDV system on the damaged beam

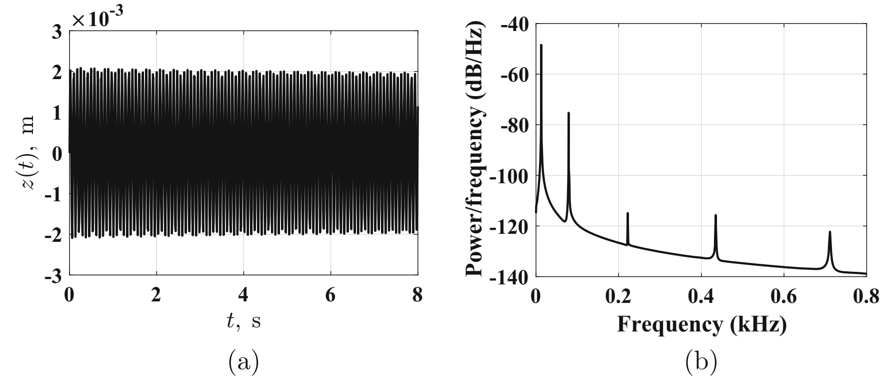

Fig. 13.3 (**a**) Response of the damaged cantilever beam at $x = 0.7$ due to the single impact at its free end and (**b**) the auto-power spectrum of the response in (**a**)

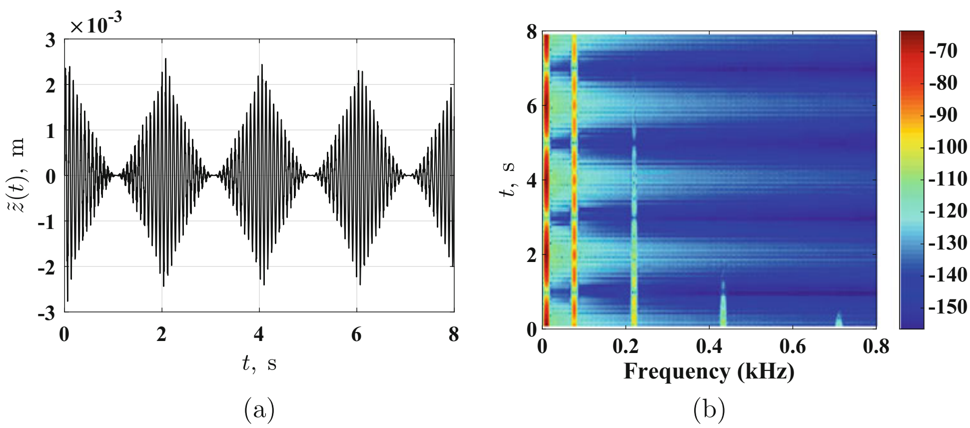

Fig. 13.4 (**a**) Response measured by the simulated CSLDV system in the first eight seconds and (**b**) a spectrogram of the response in (**a**)

spectrogram is shown in Fig. 13.4b. It can be observed that amplitudes of frequency components associated with the third through fifth modes decay faster than those with the first and second modes. Specifically, the frequency component associated with the fourth mode decays to almost zero before the second half-scan period ends and that associated with the fifth mode fast decays within the first half-scan period. Since the duration of a half-scan period is $\frac{T}{2} = 1$ s, non-zero-amplitude free response shapes of at least one half-scan period associated with the first through fourth modes can be obtained from the free response measured by the CSLDV system and that associated with the fifth mode cannot. Free response shapes obtained from the free response are shown in Fig. 13.5a–e, which correspond to the first through fifth modes, respectively. It can be seen that amplitudes of the free response shapes associated with the fourth and fifth modes of the structure decay to almost zero faster than those associated with the first three modes, which verifies the observations on the spectrogram in Fig. 13.4b.

Since there is only one non-zero-amplitude free response shape associated with the fourth mode and the free response shape associated with the fifth mode has decayed almost to zero before the end of the first half-scan period of the CSLDV system, modal damping ratios and mode shapes associated with the two modes cannot be estimated here. However, they can

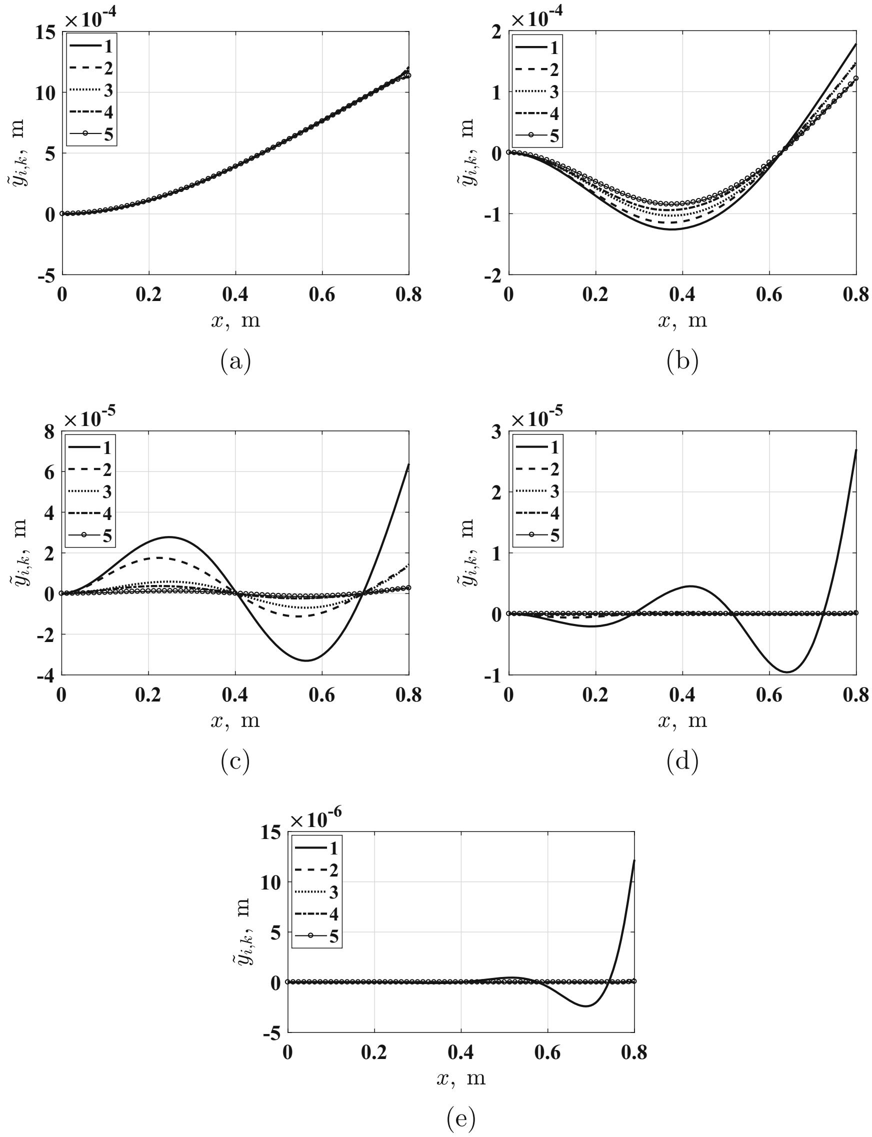

Fig. 13.5 Free response shapes of the damaged cantilever beam associated with its (**a**) first, (**b**) second, (**c**) third, (**d**) fourth and (**e**) fifth modes obtained from the response measured by the CSLDV system

be estimated if a higher scan frequency is applied so that at least two non-zero-amplitude free response shapes associated with each of the two modes can be obtained from the response measured by the CSLDV system. By applying the OMPE method in Sect. 13.2.3, modal damping ratios and mode shapes associated with the first three modes can be estimated with the obtained free response shapes here. Estimated damping ratios associated with the first three modes are listed in Table 13.1b, which compare well with those from the finite element model. Estimated mode shapes are shown in Fig. 13.6, and modal assurance criterion (MAC) values between mode shapes from the OMPE method and finite element model are above 99.99%, which indicates that the mode shapes compare well with each other. Note that the mode shapes are normalized so that they have a maximum unit amplitude.

The estimated mode shapes are then used for structural damage identification. The three mode shapes of the damaged cantilever beam are fitted by polynomials with properly determined orders. The orders of the polynomial fits are 7, 8 and 11 for the first through third mode shapes, respectively. Curvature mode shapes corresponding to the first three mode shapes and those from the polynomial fits are shown in Fig. 13.7. It can be seen that local anomaly due to the damage can be well observed by comparing the curvature mode shapes of the beam with those from the polynomial fits. CDIs corresponding to the three mode shapes are shown in Fig. 13.8a–c, and the auxiliary CDI corresponding to the three

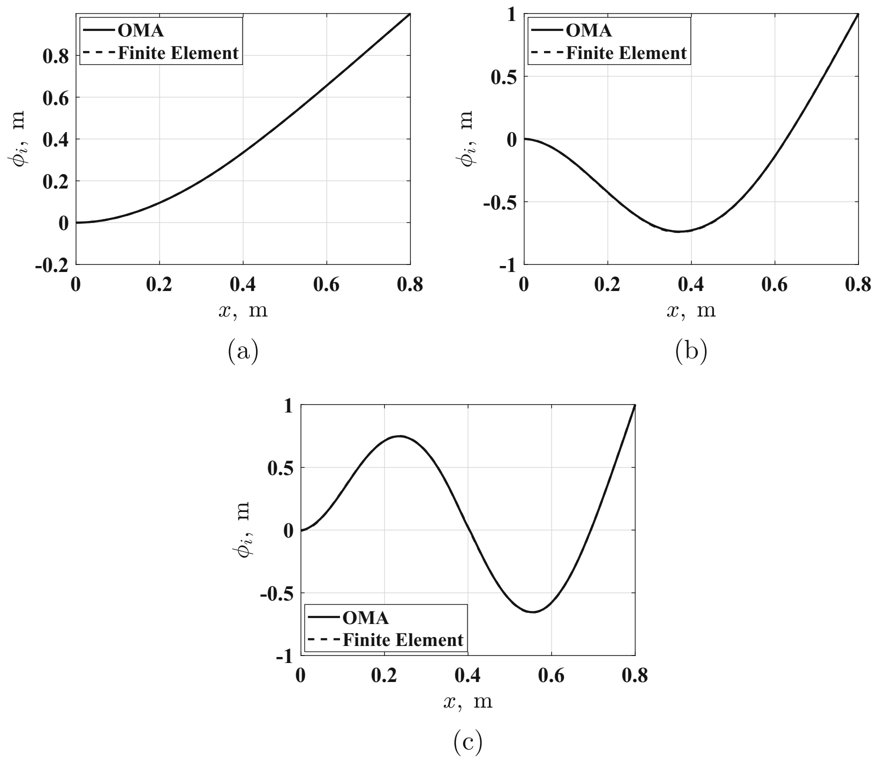

Fig. 13.6 Comparison between mode shapes of the damaged cantilever beam from the OMPE method using the free response shapes and its finite element model associated with its (**a**) first, (**b**) second and (**c**) third modes

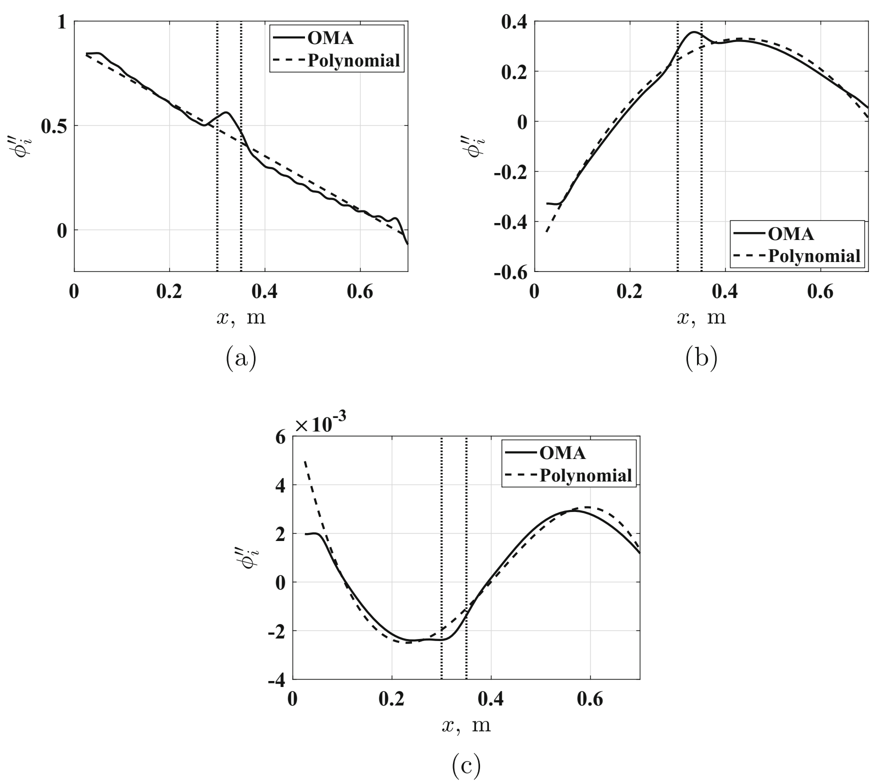

Fig. 13.7 Comparison between curvature mode shapes of the damaged cantilever beam from the OMPE method and polynomial fits associated with its (**a**) first, (**b**) second and (**c**) third modes

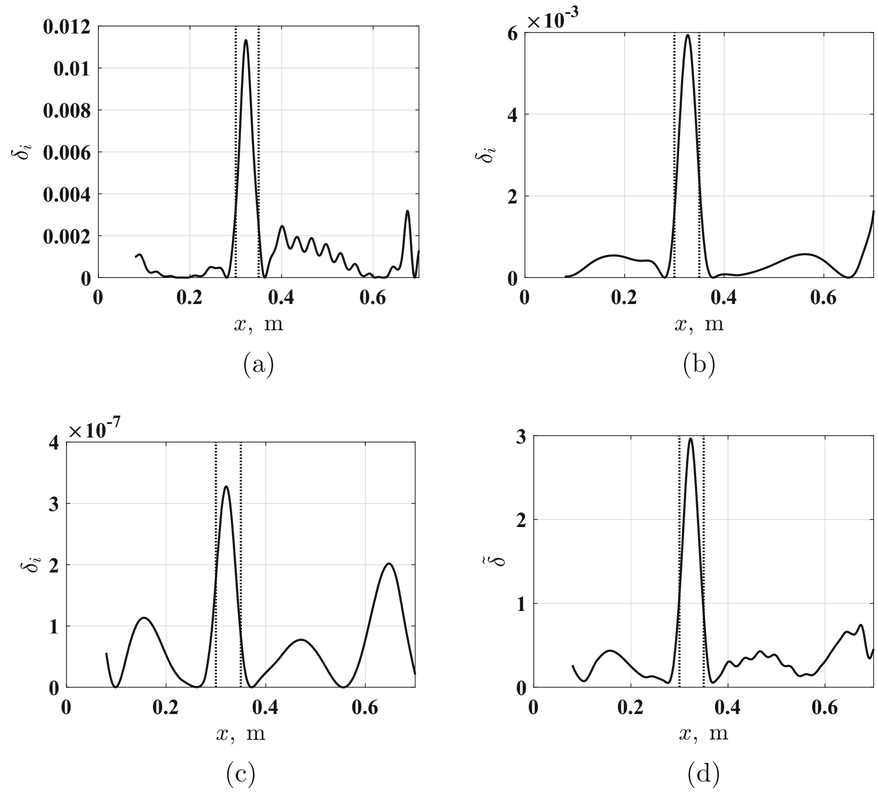

Fig. 13.8 CDIs of the damaged cantilever beam associated with its (**a**) first, (**b**) second and (**c**) third modes; (**d**) the auxiliary CDI associated with the curvature damage indices in (**a**) through (**c**). Ends of the damage are indicated by two dotted lines

damage indices is shown in Fig. 13.8d. The structural damage can be clearly and accurately identified in neighborhoods with consistently large values of the CDIs in Fig. 13.8a–c and the auxiliary CDI in Fig. 13.8d can well assist identification of the neighborhood.

13.4 Conclusions

Derivation of free response shapes of a linear, time-invariant, viscously damped structure is shown. The only current application of free response shapes is structural damage identification and they cannot be used for model validation and updating. A new OMPE method using free response measured by a CSLDV system is proposed to estimate modal parameters, including natural frequencies, modal damping ratios, and mode shapes based on the concept of free response shapes. Natural frequencies can be estimated by measuring free response of fixed points on the structure. A free response shape associated with an elastic mode corresponds to the mode shape associated with the same mode. The amplitude of the free response shape exponentially decays with a decaying rate that is directly related to the modal damping ratio and natural frequency of the mode. When the decay is compensated with an accurately estimated decaying rate, the mode shape of the mode can be automatically obtained as a result. In the proposed OMPE method, the modal damping ratio and mode shape associated with an elastic mode can be simultaneously estimated by solving an optimization problem. Free response shapes of one elastic mode in at least two half-scan periods are needed to estimate its modal damping ratio and mode shape. Using relatively low scanning frequencies can yield mode shapes of high qualities. A baseline-free method is applied to identify structural damage using mode shapes estimated by the OMPE method. In the numerical investigation, the proposed OMPE method is applied to estimate modal parameters of a viscously damped damaged beam using its free response measured by a simulated CSLDV system. Estimated modal parameters compare well with their theoretical ones and the damage can be accurately identified using the auxiliary CDI.

Acknowledgements The authors are grateful for the financial support from the National Science Foundation through Grant Nos. CMMI-1335024, CMMI-1763024, CMMI-1762917 and the College of Engineering and Information Technology at the University of Maryland, Baltimore County through a Strategic Plan Implementation Grant. The first author is also grateful for the faculty startup support from the Department of Mechanical and Materials Engineering at the University of Cincinnati.

Appendix: Short-Time Fourier Transform

The short-time Fourier transform of $\tilde{z}$, denoted by $\tilde{V}_w(t, f)$, can be expressed by

$$\tilde{V}_w(t, \omega) = \int_{-\infty}^{\infty} \tilde{z}(\tau)\, g_s^*(\tau - t)\, \mathrm{e}^{-\mathrm{j}\omega\tau} \mathrm{d}\tau \tag{13.28}$$

where g_s is a window function with a scale s, the superscript $*$ denotes complex conjugation, and $\mathrm{j} = \sqrt{-1}$. The scale s determines the width of g_s in the time domain, which should be smaller than that of a half-scan period. When $\tilde{V}_w$ at the i-th natural frequency of the structure becomes almost zero at an instant $t_{i,0}$, the amplitude of $\tilde{y}_i$ is considered to be zero. Note that in Eq. (13.28), $\tilde{V}_w(t, \omega)$ is visualized by use of a spectrogram whose intensity denotes the power spectral density associated with $\tilde{V}_w(t, \omega)$; g_s is a Hamming function that can be expressed by

$$g_s(t) = \begin{cases} 0.54 - 0.46\cos\left(\frac{2\pi t}{s}\right), & 0 \le t \le s \\ 0, & \text{otherwise} \end{cases} \tag{13.29}$$

References

1. Doebling, S.W., Farrar, C.R., Prime, M.B., et al.: A summary review of vibration-based damage identification methods. Shock Vib. Dig. **30**(2), 91–105 (1998)
2. Fan, W., Qiao, P.: Vibration-based damage identification methods: a review and comparative study. Struct. Health Monit. **10**(1), 83–111 (2011)
3. Ewins, D.J.: Modal Testing: Theory and Practice, vol. 15. Research Studies Press, Letchworth (1984)
4. Di Maio, D., Ewins, D.: Continuous scan, a method for performing modal testing using meaningful measurement parameters; Part I. Mech. Syst. Signal Process. **25**(8), 3027–3042 (2011)
5. Chen, D.-M., Xu, Y.F., Zhu, W.D.: Damage identification of beams using a continuously scanning laser doppler vibrometer system. J. Vib. Acoust. **138**(5), 051011 (2016)
6. Stanbridge, A.B., Ewins, D.J.: Modal testing using a scanning laser doppler vibrometer. Mech. Syst. Signal Process. **13**(2), 255–270 (1999)
7. Stanbridge, A.B., Ewins, D., Khan, A.: Modal testing using impact excitation and a scanning LDV. Shock Vib. **7**(2), 91–100 (2000)
8. Allen, M.S., Sracic, M.W.: A new method for processing impact excited continuous-scan laser doppler vibrometer measurements. Mech. Syst. Signal Process. **24**(3), 721–735 (2010)
9. Sriram, P., Craig, J., Hanagud, S.: A scanning laser doppler vibrometer for modal testing. Int. J. Anal. Exp. Modal Anal. **5**, 155–167 (1990)
10. Sriram, P., Hanagud, S., Craig, J.: Mode shape measurement using a scanning laser doppler vibrometer. Int. J. Anal. Exp. Modal Anal. **7**(3), 169–178 (1992)
11. Stanbridge, A.B., Ewins, D.J.: Measurement of translational and angular vibration using a scanning laser doppler vibrometer. Shock Vib. **3**(2), 141–152 (1996)
12. Yang, S., Allen, M.S.: Output-only modal analysis using continuous-scan laser doppler vibrometry and application to a 20 kw wind turbine. Mech. Syst. Signal Process. **31**, 228–245 (2012)
13. Yang, S., Allen, M.S.: Lifting approach to simplify output-only continuous-scan laser vibrometry. Mech. Syst. Signal Process. **45**(2), 267–282 (2014)
14. Wereley, N.M., Hall, S.R.: Linear time periodic systems: transfer function, poles, transmission zeroes and directional properties. In: American Control Conference, pp. 1179–1184. IEEE (1991)
15. Chen, D.-M., Xu, Y.F., Zhu, W.D.: Non-model-based multiple damage identification of beams by a continuously scanning laser doppler vibrometer system. Measurement **115**, 185–196 (2018)
16. Chen, D.-M., Xu, Y.F., Zhu, W.D.: Experimental investigation of notch-type damage identification with a curvature-based method by using a continuously scanning laser doppler vibrometer system. J. Nondestruct. Eval. **36**(2), 38 (2017)
17. Xu, Y.F., Chen, D.-M., Zhu, W.D.: Damage identification of beam structures using free response shapes obtained by use of a continuously scanning laser doppler vibrometer system. Mech. Syst. Signal Process. **92**, 226–247 (2017)
18. Meirovitch, L.: Principles and Techniques of Vibrations, vol. 1. Prentice Hall, New Jersey (1997)
19. Caughey, T., O'Kelly, M.E.: Classical normal modes in damped linear dynamic systems. J. Appl. Mech. **32**(3), 583–588 (1965)
20. Rao, S.S., Yap, F.F.: Mechanical Vibrations, vol. 4. Prentice Hall, Upper Saddle River (2011)
21. Hlawatsch, F., Auger, F.: Time-Frequency Analysis. Wiley-ISTE (2013)
22. Pandey, A., Biswas, M., Samman, M.: Damage detection from changes in curvature mode shapes. J. Sound Vib. **145**(2), 321–332 (1991)
23. Xu, Y.F., Zhu, W.D., Liu, J., Shao, Y.: Identification of embedded horizontal cracks in beams using measured mode shapes. J. Sound Vib. **333**(23), 6273–6294 (2014)